01

Empirical quality criteria for the approximation of the electronic term of a diatomic molecule by the Morse formula

© *G.S. Denisov*

St. Petersburg State University,
199034 St. Petersburg, Russia

e-mail: g.denisov@spbu.ru

A brief review of the latest results of the application of the approximation of the potential of a diatomic molecule by the Morse model function in applied spectroscopy is presented. The functions of the electronic terms of the diatomic molecules BeH, F_2, H_2, HCl, and Be_2 are compared with their two alternative approximations by the Morse function. As a criterion, we used the differences between the original (approximated) term and its Morse models, which, combined with the dependence of the anharmonicity of the original terms on the vibrational quantum number $\omega_e x_e(v)$, allowed to formulate some generalizations about the deformation of the form the original term in the approximations. Simulation always leads to an increase in the bond energy in the range of $7-50\%$ and to an increase in the number of vibrational levels. In favorable cases, the contour shape is reproduced with a deviation of no more than $100-200\,\mathrm{cm}^{-1}$ in the lower part of the potential well.

Key words: Morse formula, diatomic molecule, anharmonicity, electronic terms, vibrational structure.

1. Introduction

The Morse model potential [1], despite a very rough approximation, is widely used in molecular spectroscopy and in other areas of optics and chemical physics. According to the Chemical Abstracts Service, over 6,000 references are given on the request „Morse Formula"Ás an example, we present random selections of recent studies in the field of spectroscopy [2–13], the influence of an external field, laser dissociation of moleculescool [14–24], thermodynamics, kinetics [25–34], solid and liquid physicssti [35–44], intermolecular interactions [45–56], Morse potential properties [57–65] and v.d. [66–81]. In publications, the authors highly appreciate the usefulness of this potential [2,4,10,50,62,63,64,66], the importance is often emphasized by its mention in the titles of articles. In the university teaching of molecular spectroscopy and physical chemistry, Morse's potential is given considerable attention, including in laboratory practice, and didactic materials are regularly published in specialized journals [82–89]. At the same time, in the manuals, the question is presented according to the established standard — for example, its presentation at the stage of initial analysis [90,91] does not differ much from recent monographs and textbooks [92]. In particular, no analysis has yet been made of the distortions introduced by approximation into the shape of the potential curve and the vibrational structure of the electronic term. In this study we develop this subject, which was started in [93].

2. Problem formulation

The purpose of this study — to identify and systematize the distortions that arise during approximation, and give them a (semi)quantitative assessment.

Morse also showed in [1] that the approximation

$$U(r) = D_e \left[1 - e^{-a(r-r_e)} \right]^2, \qquad (1)$$

at which the vibrational energy $G(v)$ takes $v_\mathrm{m} + 1$ values

$$G(v) = \omega_e \left(v + \frac{1}{2} \right) - \omega_e x_e \left(v + \frac{1}{2} \right)^2,$$

$$v = 0,\, 1,\, 2,\, \ldots v_\mathrm{M}, \qquad (2)$$

can be performed in two ways, depending on the choice of initial parameters. If the bond energy D_e is unknown, it is sufficient to know the coefficients ω_e (harmonic frequency) and $\omega_e x_e$ (anharmonicity) in order to use also the known value of the equilibrium bond length r_e, find D_e and construct an electronic term (1) [93]. Let us call it $M1$. This path is used by Morse in [1] to estimate the dissociation energy of a number of molecules, the agreement with the experiment is satisfactory. If the value of D_e is known, we can use the experimental values of ω_e and D_e together with r_e to construct the term (1), we will call this term $M2$. The terms $M1$ and $M2$ constructed for a particular molecule are not identical, although they are sometimes referred to as the same. Indeed, in the $M1$ case, three reference points lie in the lower part of the potential well, and this part of the potential, and hence the vibrational levels, are reproduced

with maximum accuracy. As the energy increases, the condition of the constancy of anharmonicity for the initial term is fulfilled worse and worse, it usually increases. The vibrational levels converge faster, and the original term reaches the asymptote earlier than $M1$. The difference between their energies becomes significant, the value of D_e for $M1$ turns out to be strongly overestimated, hence false vibrational levels appear. To construct the term $M2$ in the lower part of the potential, two reference points are used, and the third determines the position of the asymptote, so that the most significant discrepancy between $M2$ and the original term occurs in its middle part and somewhat higher.

To quantify the distortions of the original term $U(r)$ introduced as a result of the approximations $M(r)$, following [94,95], we used the difference $\delta(r) \equiv U(r) - M(r)$. For several diatomic molecules, we constructed the $U(r)$ functions from high-precision theoretical data in the literature, which we considered experimental. Further we calculated the model functions $M1(r)$ and $M2(r)$ for them and the differences $\delta(r)$, as well as plotted the course of the anharmonicity coefficients $\omega_e x_e(v)$ for $U(r)$. The value of anharmonicity in [96] (formula (20.96)) is calculated from the experimental sequence of energy differences of adjacent vibrational levels (second differences):

$$G(v) - G(v - 1) = \omega(v),$$

$$\Delta_2 G(v + 1/2) = \omega(v) - \omega(v - 1) = -2\omega_e x_e. \quad (3)$$

For the Morse potential, it is constant. We can consider the variable $\omega_e x_e$ as a characteristic of the anharmonicity of some section of the potential well of the curve $U(r)$, and then the empirical function $\omega_e x_e(v)$ (or $x_e(v)$ if we exclude the individuality of the molecule) reflects the difference between the models $M1$ and $M2$ and the original term $U(r)$ [97]. Let us clarify that speaking about the anharmonicity of the original term, we mean the value of the first term of the sequence $\Delta_2 G(v)$, as is customary in the literature [98,99].

When analyzing the differences $\delta(r)$, we tried to make some generalizations of the distortions of the form $U(r)$ under Morse approximations. Anharmonicity $\omega_e x_e$ for the function $M1$ of real molecules was calculated from the experimental frequencies of transitions between vibrational levels $v = 0, 1, 2$ (by two values, $n = 2$). In the present situation it turned out to be useful to compare with the form of the anharmonicity function $\omega_e x_e(v)$, which agrees well with the details of the form of the term [93]. The complication of the form of the differences $\delta(r)$ is observed in the following sequence: a monotonic increase in anharmonicity — the existence of a minimum (first a decrease, and then an increase) — a more complicated dependence.
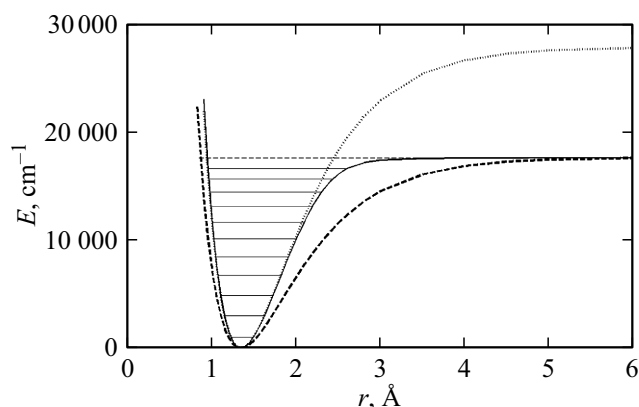
Figure 1. Potential energy curve $U(r)$ of the ground state $X\,^2\Sigma^+$ of the free radical BeH (solid curve) constructed from high-level calculated data in [102], and its Morse reconstructions $M1$ (dotted line) and $M2$ (dashed curve).

3. Results for them

3.1. Monotonic increase in anharmonicity

Differences $\delta(r)$ have the simplest form for terms in which the anharmonicity increases monotonically over a wide energy interval up to the middle of the potential well and beyond. With a large amplitude of oscillations near the asymptote, a sharp anomaly occurs due to a change in the law of interaction between atoms, an increase in the proportion of van der Waals interaction. This issue is considered in detail in the studies of Le Roy and co-authors [100,101], who modified the Morse function for a wider region by increasing the number of parameters (MorseLongRange model), but we will focus on the main part of the potential, remaining in the ideology [1] and without paying attention to the asymptotics. Let us consider the potential curves of the ground state of the free radical BeH and the F_2 molecule belonging to this group.

3.1.1. Ter,m $X^2\Sigma^+$ of the radical BeH This term is an example of the simplest Morse approximation. A rough estimate of the distortions introduced by the approximation can be made from Fig. 1, which shows the potential curves of the ground state $X^2\Sigma^+$ of the free radical BeH (solid curve) and its reconstruction $M1$ (dotted line) and $M2$ (dashed curve) constructed from high-level calculated data in [102]. The $M1$ curve reproduces well the original term in the lower part of the well up to $\sim 9000\,\mathrm{cm}^{-1}$, which is about half of its depth. Then the attraction branch goes up, the deviation from $U(r)$ increases rapidly, and its asymptote exceeds D_e by more than one and a half times. In the resulting potential well, there are false vibrational levels lying above D_e. The $M2$ curve lies below $U(r)$ on the entire section, including the repulsive branch, the deviation increases on the attraction branch, and in the upper part of the potential reaches its maximum value $\sim 5000\,\mathrm{cm}^{-1}$, and near the asymptote the curve tends to the initially assigned
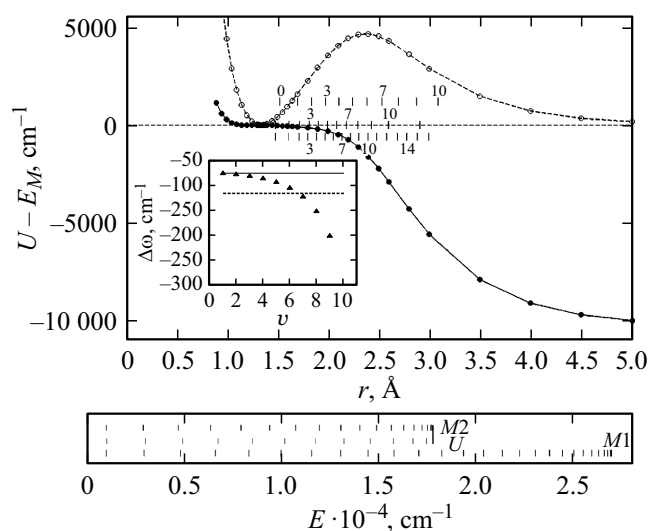
Figure 2. Differences between the potential curve $U(r)$ of the ground state $X^2\Sigma^+$ of the free radical BeH calculated with high accuracy in [102] and its Morse approximations $M1$ (solid line) and $M2$ (dashed curve). On the abscissa axis, dashes show the location of the outer classical turning points r_2 of the vibrational levels of the term $U(r)$, above and below the abscissa — the turning points r_2 of the $M1$ functions and $M2$ respectively. In the lower part of the figure, the energy scale shows the arrangement of vibrational levels for potential curves on $U(r)$, $M1$, and $M2$. The insert shows the anharmonicity $\Delta\omega(v) = \omega(v) - \omega(v-1) = -2\omega_e x_e$ of the $U(r)$ term as a function of the quantum numbers v (triangles). The straight horizontal lines show the anharmonicity constants for $M1$ (solid gray line) and $M2$ (thick dashed line).

position. It can be seen that the original function reaches the asymptote first, then $M2$, and finally $M1$. Since the potential well $M2$ is wider than $M1$, the density of vibrational levels in it should be higher.

A more accurate description of the deviations is given in the coordinates $\delta(r)$ (Fig. 2). The dashes on the abscissa show the position of the outer classical turning points r_2 ($r_2 > r_e$) for vibrational levels $U(r)$. Above and below are the values of r_2 for models $M1$ and $M2$, respectively. The additional scale in the lower part of the figure shows the position in the energy scale of the vibrational levels of the real term and approximations of $M1$ and $M2$, including for $M1$ also false levels lying above D_e. It can be seen that both repulsive branches $M1$ and $M2$ go below the original term, and its attractive branch is located between them. In the lower part of the term $U(r)$, in the interval r from 1.1 to 1.9 Å, where the approximation $M1$ satisfactorily describes the term $U(r)$, the deviation in the attraction branch slowly increases to about $200\,\mathrm{cm}^{-1}$, near level $v = 4$, $\sim 40\%$ of potential well depth $U(r)$ and $M2$ [103]. The real anharmonicity of $\omega_e x_e$ in this case increases from 37 to $43\,\mathrm{cm}^{-1}$ (insert to Fig. 2), the constant anharmonicity of the term $M1$ is equal to $37\,\mathrm{cm}^{-1}$. Further, the curve $\delta(r)$ for $M1$ quickly goes down and reaches an asymptote, where the excess of $M1$ over $U(r)$ is about $10000\,\mathrm{cm}^{-1}$, and the

real $\omega_e x_e = 150\,\mathrm{cm}^{-1}$. Due to this difference, 15 false levels were formed that lie above the asymptote. The function $\delta(r)$ for the term $M2$ forms a maximum at $r \sim 2.4$ Å near $v = 9$, at the maximum the deviation of $M2$ from the original term is greater than $4500\,\mathrm{cm}^{-1}$. On the section from $v = 9$ to the asymptote, 12% of the depth of the well, there are three levels $U(r)$ and 8 levels $M2$. Since the experimental value of D_e was used in the construction of the $M2$ function, the anharmonicity of $\omega_e x_e$ due to the higher level density should be noticeably greater than for $M1$. In this case, the condition of conservation of the harmonic frequency ω_e must also be satisfied, so that the coincidence of the asymptotes U and $M2$, marked by a vertical line on the scale in the lower part of Fig. 2, is due to an increase in the anharmonicity of $\omega_e x_e$ from 37 to $58\,\mathrm{cm}^{-1}$ due to the dimensionless multiplier x_e [97]. This is accompanied by the appearance of five false levels below the dissociation limit.

Thus, for BeH the function $M1$ satisfactorily approximates the initial term in the lower part, about 40% of the potential well, then, in the attraction branch, the deviation to higher energy increases and near the boundary of the continuous spectrum is $650\,\mathrm{cm}^{-1}$. Above the $U(r)$ asymptote, this deviation reaches the limit of $10000\,\mathrm{cm}^{-1}$, which is recorded as 55% of the addition to the bond energy of $17590\,\mathrm{cm}^{-1}$. In this case, the number of vibrational levels $M1$ in the region D_e of the initial term decreases to ten. The attraction branch of the function $M2$ already in the lower part quickly goes to a lower energy with the maximum deviation from $U(r)$ at $v = 9$ by $\sim 30\%$ from its energy. Near the last vibrational level $U(r)$ the deviation decreases to $3300\,\mathrm{cm}^{-1}$, so that only in the interval below $v = 1$ (17% of the well) the $M2$ deviation is less than $3000\,\mathrm{cm}^{-1}$, i.e. the $M2$ approximation strongly distorts the original function everywhere. In addition, the number of vibrational levels increases to 17.

3.1.2. Term $X\,{}^1\Sigma_g^+$ of the molecule F_2
The main term $X^1\Sigma_g^+$ of the molecule F_2 according to the form of the function $\delta(r)$ constructed in Fig. 3 from the data high-precision [104], is very similar to the BeH term described above, except for the repulsion branch $M1$, which is located above the real term $U(r)$, but almost merges with it at the boundary of the continuous spectrum. This feature, although confirmed by a later calculation [105], still requires a more thorough analysis. The model term $M1$ in the interval $1.3{-}1.7$ Å goes close to the potential $U(r)$ within limits not exceeding $100\,\mathrm{cm}^{-1}$. In this case, according to the insert, the vibrational levels of the $U(r)$ term converge with increasing anharmonicity $\omega_e x_e$, $12{-}14\,\mathrm{cm}^{-1}$. This region, up to $v \sim 7$ (according to [106,107] vibrational levels in total 22) is about 40% of the potential well depth $U(r)$. So this term can also be an example of the simplest term satisfactorily described by the Morse formula in the lower part of the potential. Further, the anharmonicity increases with acceleration, the attraction branch of the $M1$ curve quickly goes up (the difference
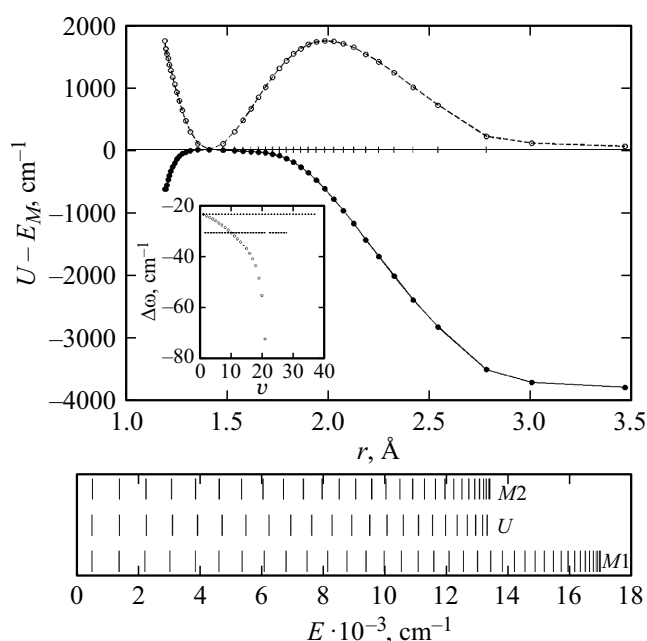
Figure 3. Differences between the potential curve $U(r)$ of the ground state $X\,^1\Sigma_g^+$ of the F_2 molecule calculated with high accuracy in [104], and its Morse approximations $M1$ (solid line) and $M2$ (dashed line). On the abscissa axis, dashes show the location of the outer classical turning points r_2 of the vibrational levels of the term $U(r)$. The insert shows the anharmonicity values $-2\omega_e x_e$ of the $U(r)$ term as a function of the quantum number v (circles), as well as the corresponding values of the anharmonicity constant for $M1$ (upper dotted line) and $M2$ (lower dashed line). In the lower part of the figure, the energy scale shows the arrangement of vibrational levels for the potential curves $U(r)$, $M1$, and $M2$.

Figure 4. Differences between the potential curve $U(r)$ of the ground state $X\,^1\Sigma_g^+$ of the hydrogen molecule H_2 calculated with a high accuracy, and its Morse approximations $M1$ (dashed line) and $M2$ (dashed line) according to the data [113]. Inserts: a — section of potential curves with the intersection of the approximation $M2$ with the potential curve $U(r)$, b — anharmonicity $-2\omega_e x_e$ of the term $U(r)$ as a function of the quantum number v, as well as the corresponding values of the anharmonicity constant for $M1$ (upper dotted line) and $M2$ (lower dashed line).

$\delta(r)$ is negative), and tends to the limit value, which is higher than the initial one by $\sim 4000\,\mathrm{cm}^{-1}$, approximately 35% of $D_e = 13400\,\mathrm{cm}^{-1}$. The $M2$ curve is located below $U(r)$, in the attraction branch the distance between them increases to the maximum value $\sim 1800\,\mathrm{cm}^{-1}$ for $r \sim 2\,\text{Å}$ ($\sim 80\%$ of the well depth, about $v = 14$), and then the curve smoothly reaches the given position of the asymptote. In the potential well, 5 false vibrational levels appear due to an increase in anharmonicity compared to $U(r)$. For $M1$ there are 16 such levels. Here also, first the original function reaches the asymptote, then $M2$, and finally $M1$. The deviation of $M2$ from $U(r)$ near its last vibrational level is $\sim 800\,\mathrm{cm}^{-1}$, so that the distortions of the term $U(r)$ when $M2$ is approximated in a wide region exceed $\sim 500\,\mathrm{cm}^{-1}$.

3.2. Terms with minimum anharmonicity

New details are found in the form of terms whose anharmonicity first decreases, passes through a minimum, and then increases monotonically. To this group belong the potential curves of the ground state of hydrogen molecules H_2 and oxygen molecules O_2 [93] (in [93] this the feature
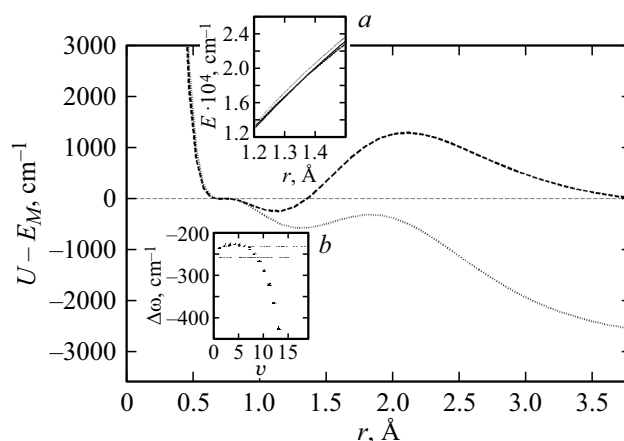
was called the anomaly of Herzberg, AH), HF and the corresponding isotopes [97]. Historically, deviations of the Morse approximation (of the $M2$ type, as can be judged from the figure) from the original term were first noted by Herzberg for the basic term of hydrogen in the book [108], where they are shown by a dotted line in Fig. 48. Below we consider in more detail the potential curves of hydrogen and HCl molecules. The latter is interesting as an intermediate case, and has also been repeatedly cited in textbooks and monographs as an example of applying the Morse approximation [96,109–112].

3.2.1. Term $X\,^1\Sigma_g^+$ of the hydrogen H_2 Figure 4 shows the differences $\delta(r)$ between the potential curve $U(r)$ of the ground state $^1\Sigma_g^+$ of the hydrogen molecule H_2 constructed from the results of a high-precision theoretical calculation [113], and Morse approximations. Terms $M1$ and $M2$ of hydrogen with vibrational structure calculated from the same data are shown in the study [93], fig. 1. The dependences $\delta(r)$ for $M1$ and $M2$ have become more complicated — in the attraction branch, both curves demonstrate a minimum, then a maximum, and after that they tend to an asymptote. The difference with $M2$ first goes below zero, after the minimum it goes up, and after crossing the x-axis near $r \sim 1.35\,\text{Å}$ it reaches a maximum. Direct intersection of terms is shown in the insert (a). This means that the curve $M2$ in the energy interval from the minimum to $\sim 20\,000\,\mathrm{cm}^{-1}$, near the level $v = 5$, goes above the term $U(r)$, i.e.reproduces AH in the same section of the potential curve. According to the insert (b), the anharmonicity decreases in this interval, and it can be assumed that this decrease serves as an empirical indication

of the deviation of the potential function $U(r)$ from the Morse formula. Real AH is about 5 times less than shown in the graph in [108]. On the $\delta(r)$ curve for $M2$, the AH appears as its negative part lying below the axis, and on the $\delta(r)$ curve for $M1$ — as a descending part from the bottom of the well to a minimum of $600\,cm^{-1}$ at $r \sim 1.35\,\text{Å}$. On the rise to the maximum at $\sim 1.85\,\text{Å}$ (a section of the well between levels 5 and 9), $M1$ converges with $U(r)$ up to about $350\,cm^{-1}$, and then their difference increases monotonically. We can assume that in the section up to $r \sim 2.2\,\text{Å}$ (approximately 70% of the depth of the well), where the average deviation is approximately $450\,cm^{-1}$, the $M1$ approximation is satisfactorily reproduces the form of the term $U(r)$. Further, the difference $\delta(r)$ goes monotonically to the asymptote $\sim 2500\,cm^{-1}$ — the excess of the extrapolated value D_e over the true value $38300\,cm^{-1}$, approximately 7%. The existence of AH somewhat narrows the potential well, which leads to a decrease in anharmonicity and to a decrease in the average deviation — in fact, to an improvement in the quality of the approximation.

In the upper part of the well, approximately from the level $v = 6$, there is a rapid increase in anharmonicity, and from this level in the mentioned Fig. 48 of the book [108] below the term $U(r)$ there is a dashed curve function $M2$, which increases the width of the potential well and the density of vibrational levels. This feature, correctly noted by Herzberg, is almost universal. For the BeH and F_2 considered above, it is this that determines the huge increase in the extrapolated value of the bond energy D_e. A slight deviation of the dotted curve on the outer side of the repulsion branch from the bottom of the well to the level $v = 1$ in Fig. 48 in [108] could not be registered.

The curve $M2$ approaches the general asymptote more slowly than the curve $U(r)$, and the curve $M1$ reaches its asymptote even later. Because of this, extra vibrational levels appear near the asymptote for the potentials $M1$ and $M2$ (in Fig. 2 in [93] one can see 4 and 3 extra levels on these terms). For the potential $M2$, the maximum deviation from the term $U(r) \sim 1500\,cm^{-1}$ is observed at $r \sim 2.1\,\text{Å}$, near the level $v = 11$, i.e at a distance (in energy) $\sim 12\%$ of the well depth from the asymptote. On the repulsion branch, the differences $\delta(r)$ for both Morse approximations $M1$ and $M2$ go up steeply and are positive, since these curves lie below the potential $U(r)$, and high in the region of the continuous spectrum acquire at zero final value.

Additional information can be obtained by changing the interval for determining the anharmonicity of the original term [93], i.e. averaging the values of $\omega_e x_e$ over several levels. Previously, averaging over three values ($n = 4$) was done in [111] for HCl, in [93] the results of averaging for H_2 and O_2. We plotted $\delta(r)$ differences for hydrogen with $\omega_e x_e$ values calculated both with $n = 2$ and with $n = 3$, 6 and 10. The most noticeable changes occur on the attraction branch of the term $M1$. An increase in the averaging interval to 3 and 6 leads successively to a weakening and almost complete disappearance of the maximum on the $\delta(r)$ curve.
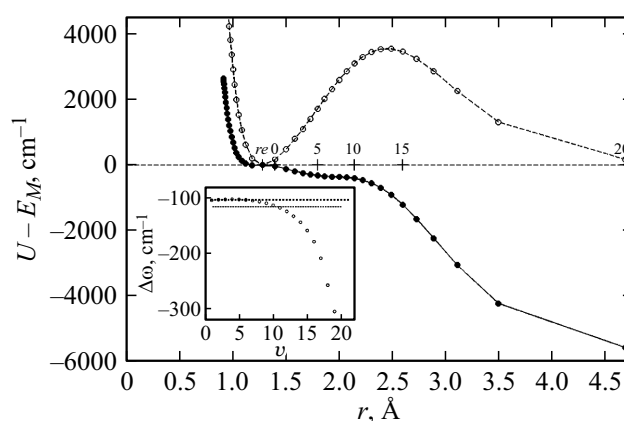

Figure 5. Differences between the potential curve $U(r)$ of the ground state $X\,^2\Sigma^+$ of the HCl molecule calculated with high accuracy in [114] and its Morse approximations $M1$ (solid line) and $M2$ (dashed lines), calculated from two vibrational frequencies ($n = 2$). On the abscissa axis, dashes show the location of the outer classical turning points r_2 of the vibrational levels of the term $U(r)$. Transitions involving $v = 18 - 20$ vibrational levels have not been observed experimentally. The insert shows the anharmonicity values $-2\omega_e x_e$ of the $U(r)$ term as a function of the quantum number v and shows the calculated anharmonicity values for $M1$ (upper dotted line) and $M2$ (lower dotted line).

At the same time, the excess of the extrapolated value D_e to $\sim 3700\,cm^{-1}$ increases. At $n = 10$ the situation changes qualitatively — D_e sharply decreases, extrema again become well expressed, the picture almost does not differ from $n = 3$. It is noteworthy that the two terms calculated with $n = 3$ and 10 intersect at $r \sim 2.0-2.1\,\text{Å}$. Obviously, these changes reflect the peculiarity of the real term, mainly AH.

3.2.2. Term $X\,^1\Sigma^+$ of the HCl molecule

The insert to Fig. 5 plots the dependence $\Delta\omega(v)$ of the differences in the vibrational frequencies of HCl according to the data [114], which shows a weakly pronounced positive AH curvature, a decrease in the value of $\Delta\omega = -2\omega_e x_e$ by $1.5\,cm^{-1}$ for $v = 5$. The dependences $\delta(r)$ have a form intermediate between hydrogen and molecules without AH, F_2 and BeH considered above. For the $\delta(r)$ branch of the attraction of the $M1$ function, a flattened section with an inflection point, but without a pronounced maximum, is observed, which is clearly visible in Fig. 4 for hydrogen. Under these conditions, in the interval r from 1 to $2.1\,\text{Å}$ (up to $v = 9$, approximately 65% of the well depth), the curve $M1$ does not move away from $U(r)$ by more than $350\,cm^{-1}$. In this interval the $M1$ model satisfactorily reproduces the real term. Further the difference rapidly increases to $5500\,cm^{-1}$.

The $\delta(r)$ $M2$ function has no features that could be associated with AH, but behaves differently from hydrogen in some details. It differs more from $M1$ not far from r_e, and the repulsion branch goes steeper than $M1$. Also a strong dome-shaped deviation of $M2$ from the term
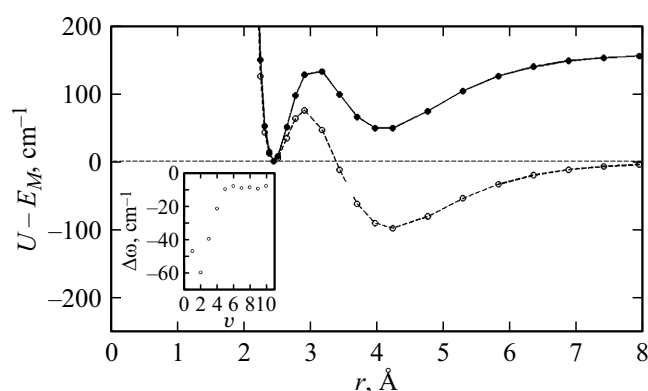
Figure 6. Functions $\delta(r)$ for the ground state $X\,^1\Sigma_g^+$ of the Be_2 molecule constructed from the data of [116]: $M1$ (solid curve), $M2$ (dashed curve). The insert shows the anharmonicity $-2\omega_e x_e$ of the $U(r)$ term as a function of the quantum number v.

$U(r)$, exceeding $1000\,\text{cm}^{-1}$, starts near $r \sim 1.7\,\text{Å}$ (near the level $v = 4$). Its maximum value $3500\,\text{cm}^{-1}$ at $v = 14$ is observed near the asymptote (at a distance of $4950\,\text{cm}^{-1}$, i.e. at $\sim 13\%$ potential well depth [114]). In the entire important region from r_e to $2.7-2.8\,\text{Å}$ the deviations of the term $M1$ from the term $U(r)$ are smaller than those of the term $M2$. The extrapolated $M1$-value of the bond energy D_e per $5500\,\text{cm}^{-1}$, i.e. by $\sim 15\%$, exceeds the real value of $37214\,\text{cm}^{-1}$. The authors reviewing this example give a close excess value of — 17% [96], 15% [110], 20% [112].

3.3. Noticeable deviations in the form of the potential curve from the traditional

form

Deviations can be caused by features of the electronic structure, such as Be_2, or perturbations, such as „avoided crossing" (avoided crossing, a typical example — the ground state of alkali halide molecules). We consider the term $X\,^1\Sigma_g^+$ of the ground state of the Be_2 molecule, which is also of interest because for it Merritt and co-authors compared with Morse approximation $M2$ [115].

3.3.1. Term $X\,^1\Sigma_g^+$ of the molecule F_2 Figure 6 shows the differences $\delta(r)$ between the term $U(r)$ calculated from high precision theoretical data [116] and its interpretations $M1$ and $M2$. These differences have a specific form, which is very different from the examples considered above. The specificity of the ground state of Be_2 is that, under vibrational excitation, already at $v > 4-5$ (11 levels in total), the electronic structure of the molecule is rearranged in such a way that the covalent interaction near the external turning point becomes van der Waals dispersive [117]. This uniqueness manifests itself in the arrangement of vibrational levels and in the unusual form of the $\delta(r)$ function. According to [93,115,118], the Burge−Sponer (B−Sh) [119,120] diagram has the form of two straight line segments located at an angle, which is

generally characteristic of preventing the intersection of two electronic terms, but here the reason is another. It was found in the studies [115,118] that in the first section of the B−Sh diagram, up to the break near $r = 4\,\text{Å}$, near $v = 4$, the connection is well described by the Morse potential, but in the second section, the dependence is more complex. Merritt et al. [115] in Fig. 3 showed the original term Be_2 $X\,^1\Sigma_g^+$ and its approximation by a Morse function of type $M2$. The graph shows the intersection of terms at $r = 3.1\,\text{Å}$ near $v = 2$, and in the lower part of the potential, the function $M2$ lies on the outside — similar to AH, but with the opposite sign. This feature leads to the formation of the maximum of the $\delta(r)$ $M2$ function in the positive region and its reaching zero value near $r = 3.4\,\text{Å}$ followed by the formation of a minimum in the negative region at $r = 4.1\,\text{Å}$ in the region of the B−Sh graph break. An analysis of the second differences in [93] (insert in Fig. 4) showed one more section on the Be_2 electronic term up to $r\ 3.1\,\text{Å}$ (near the level $v = 2$), at which the anharmonicity increases (AH vice versa). In the second section up to $r \sim 4\,\text{Å}$ (near the $v = 5$ level), the anharmonicity of $\omega_e x_e$ drops sharply from 30 to $5\,\text{cm}^{-1}$, and then it remains approximately constant up to $\sim 1\,\text{cm}^{-1}$ (third segment). The curve $M1$ constructed with high anharmonicity for $n = 2$ goes to the limit $751\,\text{cm}^{-1}$ (Table 1 in the study [118]), which is $180\ \text{cm}^{-1}$ below the real bond energy $930\,\text{cm}^{-1}$ [118]. Therefore, the approximation $M1$ corresponds to the positive value of the function $\delta(r)$, and the extrema of $\delta(r)$ $M1$ coincide with $M2$.

4. Conclusion

The Morse molecule, which does not exist in nature, together with the non-existent abstract harmonic frequency ω_e, represent the first anharmonic approximation with constant anharmonicity $\omega_e x_e$, for which, by happy coincidence, the Schr?dinger equation is solved almost strictly. Therefore, the Morse molecule serves as a convenient initial object in the study of many phenomena in various fields of chemical physics. Kaplan [121] believes that the Morse potential is widely used, in particular, in the study of the properties of crystals, because „the properties of crystals are most sensitive in the range of distances in which the Morse potential quite satisfactorily describes the real potential curve". An attempt [122] to add a cubic term with a second anharmonicity coefficient to the series (2) does not seem to be developed.

When approximating the term $U(r)$ by the Morse function, it is important to know the type and magnitude of the introduced distortions, and their complete characteristic is given by the difference $\delta(r) \equiv U(r) - M(r)$. The empirical dependence $\omega_e x_e(v)$ of the second energy differences of successive vibrational levels of the term $U(r)$, which characterizes the dependence of the anharmonicity on the position of the level in the potential well, is of great use for analysis. The function $\omega_e x_e(v)$ can be considered as a formal

second approximation after ω_e (harmonic approximation, $x = 1$) and $\omega_e x_e = C$ (the simplest anharmonic Morse approximation). In terms of the shape of the potential curve — parabola, one constant (ω_e); Morse contour, two constants (ω_e, $\omega_e x_e$); real molecule, set (ω_e, $\omega_e x_e(v)$ and $\delta(r)$).

5. Conclusions

In formulating the conclusions, it should be added that they are based on very limited material and can be noticeably clarified in the future. In particular, qualitatively new generalizations can be expected after a more detailed study of molecules containing isotopes, mainly hydrogen isotopes [97].

The expediency of using the empirical dependence of the difference of functions $U(r) - M(r)$, where $U(r)$ — is the original term, and $M(r)$ — is the Morse approximation $M1$ or $M2$, to quantify the distortions of the real term of a diatomic molecule with a valence bond and its vibrational structure as a result of approximation.

The usefulness of using the empirical anharmonicity dependence $\omega_e x_e(v)$ as an auxiliary criterion for the presence of singularities in the shape of the lower part of the potential curve is shown.

A monotonic increase in anharmonicity correlates with the simplest form of $M(r)$, while an anomalous decrease for several initial levels leads to its complication.

In favorable cases it is possible to obtain a satisfactory approximation of $M1$ with an average difference (upwards in energy) from the original term $100-200\,\text{cm}^{-1}$ in the lower part of $40-50\%$ of the potential wells. Approximation $M2$ gives significant deviations (more than $500-1000\,\text{cm}^{-1}$ towards lower energy) almost at the entire depth of the well.

Approximation $M1$ usually leads to an increase in the depth of the potential well to $\sim 50\%$ or more and to its narrowing in the region of bound states of the term $U(r)$ — in this region the number of vibrational levels decreases (compared to the number of vibrational levels of the term $U(r)$). For the $M2$ approximation, the well width increases and the number of vibrational levels increases accordingly.

Approximations $M1$ and $M2$ lead to the appearance of false vibrational levels. False levels are adjacent to the asymptote of the original term: approximation levels $M1$ — from the side of the continuous spectrum, levels of approximation $M2$ — from the side of the discrete spectrum.

The described results refer to molecules with a valence bond. It follows from the examples given in the study [93] that in van der Waals molecules the anharmonicity changes according to a different law. This issue requires special consideration.

We would like to hope that the above information will help specialists who use the Morse formula to approximate the real term to optimize their working conditions, and teachers will be given the opportunity to offer students new tasks.

Note: Herzberg and Oui [123] in describing the results of a precision study of the emission spectrum of hydrogen H_2 give the dependences $G_1(v)$ and $\Delta_2 G(v)$ (the last one in Fig. 8 from [123] almost exactly coincides with our insert (b) in Fig. 4), and their phrase in the conclusion „It would be interesting to carry out a theoretical analysis that would give a more detailed explanation of the behavior of the B_v and ΔG curves at low values v" (meaning AH) acquires additional relevance due to indicated by the prevalence of this phenomenon.

Conflict of interest

The author declares that he has no conflict of interest.

References

[1] P.M. Morse. Phys. Rev., **34** (1), 57 (1929).

[2] A. Durmus, A. Ozfidan. Chem. Phys., **543** (11), 111078 (2021). DOI:10.1016/j.chemphys.2020.111078

[3] I. Amila, M.J. Idrissi, A. Fedoul, S. Sayouri. IOP Conf. Ser.: Mater. Sci. Eng., **1160**, 012003 (2021). DOI: 10.1088/1757-899X/11601/012003

[4] T. Begušić, J. Vaníček. J. Chem. Phys., **153** (18), 184110 (2020). DOI:10.1063/5.0031216

[5] M. Al-Raaei, M.S. El-Daher. AIP Advances, **10** (03), 035305 (2020). DOI:10.1063/1.5113593

[6] R. Lemus. J. Math. Chem., **58** (1), 29 (2020). DOI: 10.1007/s10910-019-01071-8

[7] L.D. Smith, A.G. Dijkstra. J. Chem. Phys., **151** (16), 164109 (2019). DOI: 10.1063/1.5122896.

[8] A. Anda, D. Abramavicius, T. Hansen. Phys. Chem. Chem. Phys., **20** (3), 1642 (2018). DOI: 10.1039/c7cp06583c

[9] M. Micciarellia, R. Conte, J. Suarez, M. Ceotto. J. Chem. Phys., **149** (6), 064115 (2018). DOI: 10.1063/1.5041911

[10] W.L. Smith. J. Mol. Spectr., **316**, 105 (2015). DOI:10.1016/j.jms.2015.06.007

[11] T. Hirano, M.B.D. Andaloussi, U. Nagashima, P. Jensen. J. Chem. Phys., **141** (9), 094308 (2014). DOI: 10.1063/1.4892895

[12] A. Bordoni, N. Manini. Int. J. Quant. Chem., **107** (4), 782 (2007). DOI: 10.1002/qua.21189

[13] I. Nasser, M.S. Abdelmonem, H. Bahlouli, A.D. Alhaidari. J. Phys. B, **40** (21), 4245 (2007). DOI: 10.1088/0953-4075/40/21/011

[14] M.D. Forlevesi, R.E. de Carvalho, E.F. de Lima. Phys. Rev. E, **104** (1), 014206 (2021). DOI: 10.1103/PhysRevE.104.014206

[15] J.F. Triana, F.J. Hernández, F. Herrera. J. Chem. Phys., **152** (23), 234111 (2020). DOI:10.1063/5.0009869

[16] H.S. Alqannas, S. Abdel-Khalek. Optical & Quantum Electronics, **51** (2), 50 (2019). DOI: 10.1007/s11082-019-1753-8

[17] J. Svensmark, O.I. Tolstikhin, L.B. Madsen. Phys. Rev. A, **97** (03), 033408 (2018). DOI: 10.1103/PhysRevA.97.033408

[18] M.T. Lee, A. Vishnyakov, A.V. Neimark. J. Chem. Theory Comp., **11** (9), 4395 (2015). DOI: 10.1021/acs.jctc.5b00467

[19] S. Sowlati-Hashjin, C.F. Matta. J. Chem. Phys., **139** (14), 144101 (2013). DOI: 10.1063/1.4820487

[20] E.F. de Lima, R.E. de Carvalho. Physica D, **241** (20), 1753 (2012). DOI:10.1016/j.physd.2012.08.001

[21] A. Sethi, S. Keshavamurthy. Mol. Phys., **110** (9-10), 717 (2012). DOI:10.1080/00268976.2012.667166

[22] V.A. Astapenko, M.S. Romadanovskii. J. Exp. Theor. Phys., **110** (3), 376 (2010). DOI: 10.1134/S1063776110030027

[23] A. Sethi, S. Keshavamurthy. Phys. Rev. A, **79** (3), 033416 (2009). DOI: 10.1103/PhysRevA.79.033416

[24] E.F. de Lima, J.E.M. Hornos. J. Phys. A, **38** (7), 815 (2005). DOI:10.1088/0953-4075/38/7/004

[25] T. Gautie, J.P. Bouchaud, P. Le Doussal. J. Phys. A, **54** (25), 255201 (2021). DOI: https://doi.org/10.1088/1751-8121/abfc7f.

[26] I.S. Gomez, E.S. Santos, O. Abla. Modern Phys. Lett. A, **36** (20), 2150140 (2021). DOI: 10.1142/S0217732321501406

[27] K. Chabi, A. Boumali. Revista Mexicana de Fisica, **66** (1), 110 (2020). DOI: 10.31349/RevMexFis.66.110

[28] S.L. Tang, Y. Wang, Q.Y. Xia, X.H. Ju. J. Chem., Article ID 7512737 (2020). https://doi.org/10.1155/2020/7512737.

[29] M. Wan, J. Song, W. Li, L. Gao, W. Fang. J. Comput. Chem., **41** (8), 814 (2020). DOI: 10.1002/jcc.26131

[30] I.V. Likhachev, V.D. Lakhno. Chem. Phys. Lett., **727**, 55 (2019). DOI:1016/j.cplett.2019.04.027

[31] B.A. Mamedov, H. Cacan. Contributions to Plasma Phys., **59** (9), e201900021 (2019). DOI: 10.1002/ctpp.201900021

[32] H. Cacan, B.A. Mamedov. J. Chem. Thermodyn., **138**, 147 (2019). DOI: 10.1016/j.jct2019.06.015.

[33] V. Rui Zhao, D. Gao, X. Pan, W. Xia, H. Yu, S. Yu, L. Yao. Chem. Phys. Lett., **703**, 97 (2018). DOI: 10.1016/j.cplett.2018.05.018

[34] M. Buchowiecki. Chem. Phys. Lett., **687**, 227 (2017). DOI: 10.1016/j.cplett.2017.09.025

[35] J.M. Hu, J.P. Zhai, F.M. Wu, Z.K. Tang. J. Phys. Chem. B, **114** (49), 16481 (2010).DOI:10.1021/jp1076615

[36] E. Benassi. Chem. Phys., **515**, 323 (2018). https://doi.org/10.1016/j.chemphys.2018.09.005

[37] O. Ortíz, M. Esmann, N.D. Lanzillotti-Kimura. Phys. Rev. B, **100** (8), 085430 (2019). DOI: 10.1103/PhysRevB.100.085430.

[38] S. Kim, S.N. Hood, A. Walsh. Phys. Rev. B, **100** (4), 041202 (2019). DOI: 10.1103/PhysRevB.100.041202.

[39] N.V. Hung, D.Q. Vuon. Modern Phys. Lett. B, **33** (20), 1950237 (2019). DOI: 10.1142/S021798491950237.

[40] T. Morimoto, M. Nagai, Y. Minowa, M. Ashida, Y. Yokotani, Y. Okuyama, Y. Kani. Nature Communications, **10** (1), 1 (2019). Article number 2662. https://doi.org/10.1038/s41467-019-10501-9.

[41] N.B. Duc, V.Q. Tho. Physica B, **552**, 1 (2019). DOI: 10.1016/j.physb.2018.09.038.

[42] D.D. Abajingin. Advances in Physics. Theories and Applications, **8**, 36 (2012).

[43] R.S. McEntire, Y.L. Shen. Int. J. Mech. Mater. Des., **4** (4), 361 (2008). DOI: 10.1007/s10999-008-9060-8

[44] K. Mylvaganam, L.C. Zhang. Nanotechnology, **13** (5), 623 (2002). DOI: 10.1088/0957-4484/13/5/316

[45] G. Kacar, G. With. J. Mol. Liq., **302** (11), 112581 (2020). DOI: 10.1016/j.molliq.2020.112581.

[46] J.N. Scott, J.M. Vanderkooi. Water. **2**, 14 (2010). DOI: 10.14294/WATER.2010.1

[47] A. Matsumoto. Z. Naturforsch. A, **66**a (12), 774 (2011). DOI: 10.5560/ZNA.2011-0042

[48] E. de Oliveira Martins, V.B. Barbosa, G. Weber. Chem. Phys. Lett., **715**, 14 (2019). DOI: 10.1016/j.cplett.2018.11.015.

[49] S.V. Goryainov. Physica B, **407** (21), 4233 (2012). DOI: 10.1016/j.physb.2012.06.045

[50] L. Yang, L. Sun, W.Q. Deng. J. Phys. Chem. A, **122** (6), 1672 (2018). DOI: 10.1021/acs.jpca.7b11252.

[51] A. Vishnyakov, R. Mao, M.T. Lee, A.V. Neimark. J. Chem. Phys., **148** (2), 024108 (2018). DOI: 10.1063/1.4997401.

[52] K.P. Santo, A. Vishnyakov, R. Kumar, A.V. Neimark. Macromolecules, **51** (14), 4987 (2018). DOI: 10.1021/acs.macromol.8b00493.

[53] S. Zdravković, A.N. Bugay, A.N. Parkhomenko. Nonlinear Dyn., **90** (4), 2841 (2017). DOI 10.1007/s11071-017-3845-y

[54] M.T. Lee, A. Vishnyakov, A.V. Neimark. J. Chem. Phys., **144** (1), 014902 (2016). DOI: 10.1063/1.4938271

[55] M.A. Boyer, A.B. McCoy. J. Chem. Phys., **156** (5), 054107 (2022). DOI: 10.1063/5.0080892

[56] A. Vishnyakov, D.S. Talaga, A.V. Neimark. J. Phys. Chem. Lett., **3** (21), 3081 (2012). DOI: 10.1021/jz301277b.

[57] A. Belfakir, E.M.F. Curado, Y. Hassouni. Annals of Physics, **423**, 168331 (2020). DOI: 10.1016/j.aop.2020.168331.

[58] T.C. Lim, J.A. Dawson. Mol. Phys., **116** (9), 1127 (2018). DOI: /10.1080/00268976.2017.1407003.

[59] T. Urbanczyk, J. Koperski. Chem. Phys. Lett., **640**, 82 (2015). DOI: 10.1016/j.cplett.2015.10.013

[60] T. Urbanczyk, M. Strojecki, A. Pashov, A. Kedziorski, P. Zuchowski, J. Koperski. J. Phys. Conf. Ser., **810**, 012018 (2017). DOI: 10.1088/1742-6596/810/1/012018

[61] S. Xantheas, J.C. Werhahn. J. Chem. Phys., **141** (6), 064117 (2014). DOI: 10.1063/1.4891819.

[62] P.Q. Wang, L.H. Zhang, C.S. Jia, J.Y. Liu. J. Mol. Spectr., **274**, 5 (2012). DOI: 10.1016/j.jms.2012.03.005.

[63] M. Angelova, V. Hussin. J. Phys., A, **41** (7), 304016 (2008). DOI: 10.1088/1751-8113/45/24/244007

[64] A. Leonard, S. Deffner. Chem. Phys., **446**, 18 (2015). DOI: 10.1016/j.chemphys.2014.10.020

[65] A.M. Desai, N. Mesquita, V. Fernandes. Physica Scripta, **95** (8), 085401 (2020). DOI: 10.1088/1402-4896/ab9bdc

[66] L. Yang, L. Sun, W.Q. Deng. J. Phys. Chem. A, **123** (36), 7847 (2019). DOI: 10.1021/acs.jpca.9b02055.

[67] C.A. Latorre, J.P. Ewen, C. Gattinoni, D. Dini. J. Phys. Chem. B, **123** (31), 6870 (2019). DOI: 10.1021/acs.jpcb.9b02925.

[68] A.C. Lasaga, T. Otake, Y. Watanabe, H. Ohmoto. Earth and Planetary Science Letters, **268** (1-2), 225 (2008). DOI: 10.1016/j.epsl.2008.01.016.

[69] M.B. Yeamin, N. Faginas-Lago, M. Albertı, I.G. Cuesta, J. Sanchez-Marın, A.M.J. Sanchez de Meras. RSC Advances, **4** (97), 54447 (2014). DOI: 10.1039/c4ra08487j.

[70] J. Récamier, W.L. Mochán. Mol. Phys., **107** (14), 1467 (2009). DOI: /10.1080/00268970902942268.

[71] Y. Shim, H.J. Kim. J. Chem. Phys., **125** (2), 024507 (2006). DOI : 2060/10.1063/1.2206579.

[72] M.L. Strekalov. Chem. Phys. Lett., **419** (1−3), 1 (2006). DOI: 10.1016/j.cplett.2005.11.042.

[73] A. Chenaghlou, S. Aghaei, N.G. Niari. Eur. Phys. J. D, **75** (4) 139 (2021). DOI:10.1140/epjd/s10053-021-00156-x

[74] A.A. Medvedev, V.V. Meshkov, A.V. Stolyarov, M.C. Heaven. Phys. Chem. Chem. Phys., **20** (40), 25974 (2018). DOI: 10/1039/c8cp04397c.

[75] J. Provazza, R. Tempelaar, D.F. Coker. J. Chem. Phys., **155** (1), 014108 (2021). DOI: 10.1063/5.0053735.

[76] M.D. Garcia, A.S. de Castro, P. Alberto, L.B. Castro. Physics Letters A, **381** (25−26), 2050 (2017). DOI: 10.1063/5.0031216

[77] P. Bornhauser, M. Beck, Q. Zhang, G. Knopp, R. Marquardt, C. Gourlaouen, P.P. Radi. J. Chem. Phys., **153** (24), 244305 (2020). DOI: 10.1063/5.0028908

[78] R.G. Pingak, A.Z. Johannes, Z.S. Ngara, M. Bukit, F. Nitti, D. Tambaru, M.Z. Ndii. Results in Chemistry, **3** (1), 100204 (2021). DOI: 10.1016/j.rechem.2021.100204

[79] A.Z. Li, W.G. Harter. Chem. Phys. Lett., **633**, 208 (2015). DOI: 10.1016/j.cplett.2015.05.035

[80] D. Mikulski, K. Eder, J. Konarski. J. Math. Chem., **52** (6), 1552 (2014). DOI: 10.1007/s10910-014-0335-z.

[81] S.V. Krasnoshchekov, X. Chang. Int. Rev. Phys. Chem., **38** (1), 63 (2019). DOI: 10.1080/0144235X.2019.1593583

[82] S.B. Bayram, M.V. Freamat. Amer. J. Phys., **80** (8), 663 (2012). doi: 10.1119/1.4722793

[83] J.C. Williamson. J. Chem. Educ., **84** (8), 1355 (2007). Also Suppl. Mat. DOI: 10.1021/ed084p1355

[84] J. Zúñiga, A. Bastida, A. Requena. J. Chem. Educ., **85** (12), 1675 (2008). DOI: 10.1021/ed085p1675

[85] K.F. Lim, W.F. Coleman. J. Chem. Educ., **82** (8), 1263 (2005). DOI: 10.1021/ed082p1263.2

[86] J.D. Gaynor, A.M. Wetterer, R.M. Cochran, E.J. Valente, S.G. Mayer. J. Chem. Educ., **92** (6), 1081 (2015). DOI: 10.1021/ed5004965

[87] P.D. Cooper. J. Chem. Educ., **87** (7), 687 (2010). DOI: 10.1021/ed100287r

[88] S. Ghosh, M.K. Dixit, S.P. Bhattacharyya, B.L. Tembe. J. Chem. Educ., **90** (11), 1463 (2013). DOI: 10.1021/ed4002199

[89] J.C. Williamson, T.S. Kuntzleman, R.A. Kafader. J. Chem. Educ., **90** (3), 383 (2013). DOI: 10.1021/ed300455n

[90] L. Pauling, E.B. Wilson. *Introduction to Quantum Mechanics With Applications to Chemistry*, McGraw Hill Book Company, New York, 1935.

[91] H.B. Dunford. *Elements of Diatomic Molecular Spectra*, Addison-Wesley Publ. Co, Reading, Massachusetts, 1968.

[92] M. Diem. *Quantum Mechanical Foundations of Molecular Spectroscopy*, 1st Ed., Wiley-VCH, Weincheim, Germany, 2021.

[93] G.S. Denisov, I.G. Denisov. Spectr. Acta A, **262** (12), 120111 (2021). DOI: 10.1016/j.saa.2021.120111

[94] A.A. Zavitsas. J. Mol. Spectr., **236** (2), 168 (2006). DOI: 10.1016/j.jms.2006.01.008

[95] H.Y. Abdullah. Bull. Mater. Sci., **42** (142) 1 (2019). DOI: 10.1007/s12034-019-1824-2

[96] M. A. Yeliashevich. *Molekulyarnaya spektroskopiya*, KOMOKniga, 2-e izd. 2007. (in Russian).

[97] G.S. Denisov, K.G. Tokhadze. Opt. i spectr., **129** (11), 1375 (2021). DOI: 10.21883/OS.2021.11.51635.2483-21.

[98] K.P. Huber, G. Herzberg, *Molecular Spectra and Molecular Structure IV. Constants of Diatomic Molecules*, Van Nostrand Reynolds, New York, 1979.

[99] CRC *Handbook of chemistry and physics*, Ed. David R. Lide, 87th ed, Section 9, Spectroscopic Constants of Diatomic Molecules, pp. 9−82, CRC Press, Boca Raton, FL, 2006.

[100] R.J. Le Roy. Determining Equilibrium Structures and Potential Energy Functions for Diatomic Molecules, Ch. 6, in: *Equilibrium Molecular Structures*, Eds: J. Demaison, J. E. Boggs, A. G. Csaszar. CRC Press, 2011, p. 159−204.

[101] R.J. Le Roy, C.C. Haugen, J. Tao, H. Li. Mol. Phys., **109** (3), 435 (2011). DOI: 10.1080/00268976.2010.52734.

[102] J. Koput. J. Chem. Phys., **135** (24), 244308 (2011). DOI: 10.1063/1.3671610

[103] R.J. Le Roy, D.R.T. Appadoo, R. Colin, P.F. Bernath. J. Molec. Specr., **236** (2), 178 (2006). DOI: 10.1016/j.jms.2006.01.010

[104] L. Bytautas, N. Matsunaga, T. Nagata, M.S. Gordon, K. Ruetenberg. J. Chem. Phys., **127** (20), 204301 (2007). DOI: 10.1063/1.2801989

[105] S. Chattopadhyay, U.S. Mahapatra, R.K. Chaudhuri. Mol. Phys., **112** (20), 2720 (2014). DOI: 10.1080/00268976.2014.906675

[106] L. Bytautas, N. Matsunaga, T. Nagata, M.S. Gordon, K. Ruetenberg. J. Chem. Phys., **127** (20), 204313 (2007). DOI: 10.1063/1.2805392

[107] E.A. Colbourn, M. Dagenais, A.E. Douglas, J.W. Raymonda. Can. J. Phys., **54** (13), 1343 (1976).

[108] G. Herzberg. *Molecular Spectra and Molecular Structure I. Diatomic Molecules*, New York, 1939.

[109] S. Flugge, Practical Quantum Mechanics, Springer, NY, 1974, v. 1, p. 182.

[110] B.W. Moore, *Basic Physical Chemistry*, Prentice-Hall, Englewood Cliffs, N.J., 1983, p. 589.

[111] S.K. Dogra, H.S. Randhava, *Molecular Spectroscopy*, McGraw-Hill, 2012, p. 94−100.

[112] R.K. Hanson, R.M. Spearrin, C.S. Goldenstein, *Spectroscopy and Optical Diagnostics of Gases*, Springer, 2016, p. 52.

[113] L. Wolniewicz. J. Chem. Phys., **99** (3), 1851 (1993). DOI: 10.1063/1.465303

[114] J.A. Coxon, P.G. Hadjigeorgiou. J. Quant. Spectr. Rad. Trans., **151**, 133 (2015). DOI: 10.1016/j.jqsrt.2014.08.028

[115] J.M. Merritt, V.E. Bondybey, M.C. Heaven. Science, **324** (5934), 1548 (2009). DOI: 10.1126/science.1174326

[116] M. Lesiuk, M. Przybytek, J.G. Balcerzak, M. Musial, R. Moszynski. J. Chem. Theory Comput., **15** (4), 2470 (2019). DOI: 10.1021/acs.jctc.8b00845

[117] A.V. Mitin. Chem. Phys. Lett., **682**, 30 (2017). DOI: 10.1016/j.cplett.2017.05.071

[118] A.B. McCoy, Chem. Phys. Lett., **501** (4−6), 603 (2011). DOI: 10.1016/j.cplett.2010.11.065

[119] R.T. Birge, H. Sponer. Phys. Rev., **28** (2), 259 (1926).

[120] A.G. Gaydon, *Dissociation Energies and Spectra of Diatomic Molecules.* 2d Ed. Chapman & Hall, L. 1968.

[121] I.G. Kaplan, *Intermolecular Interactions*, Wiley, Chichester, 2006. P. 191.

[122] M.N. Angelova, V.K. Dobrev, A. Frank. Eur. Phys. J. D, **31** (1), 27 (2004) DOI: 10.1140/epjd/e2004-00111-6

[123] G. Herzberg, L.L. Howe. Can. J. Phys., **37** (5), 636 (1959).